Food and Chemical Toxicology 134 (2019) 110804

Contents lists available at ScienceDirect

Food and Chemical Toxicology

journal homepage: www.elsevier.com/locate/foodchemtox

Role of ATP-sensitive potassium channels and inflammatory response of basilar artery smooth muscle cells in subarachnoid hemorrhage of rabbit and immune-modulation by shikonin

Xianqing Shi[a,*], Lirong Zhen[a], Hao Ding[b], Jing Chen[a], Songsong Zhang[a], Yongjian Fu[a]

[a] Intensive Care Unit, Guizhou Provincial People's Hospital, Guiyang, Guizhou Province, 550002, China
[b] Intensive Care Unit, Guizhou Provincial Orthopedics Hospital, Guiyang, Guizhou Province, 550007, China

ARTICLE INFO

Keywords:
Subarachnoid hemorrhage
Basilar artery smooth muscle cells
ATP-Sensitive potassium channels current
Traditional Chinese medicine

ABSTRACT

Objective: To investigate the role of inflammatory response, oxidative damage and changes of ATP-sensitive potassium channels (sK_{ATP}) in basilar artery (BA) smooth muscle cells (SMCS) of rabbits in subarachnoid hemorrhage (SAH) model.

Methods: Time course studies on inflammatory response by real-time PCR, oxidative process and function of isolated basilar artery after SAH in New Zealand White rabbits were performed. Basilar artery smooth muscle cells (BASMCs) in each group were obtained and whole-cell patch-clamp technique was applied to record cell membrane capacitance and K_{ATP} currents. The morphologies of basal arteries were analyzed. Protective effect of shikonin were also determine by same parameters.

Results: Inflammatory cytokines levels were highest at 24h compare to 72h after SAH whereas the oxidative damage and cell death marker were at highest peak at 72h. Oxidative damage peak coincided with significant alterations in cell membrane capacitance, K_{ATP} currents and morphological changes in basilar arteries. Shikokin pretreatment attenuated early inflammatory response at 24h and associated oxidative damage at 72h. Finally, shikonin attenuated morphological changes in basilar arteries and dysfunction.

Conclusion: Currents of ATP-sensitive potassium channels in basilar smooth muscle cells decreased after SAH by putative oxidative modification from immediate inflammatory response and can be protected by shikonin pretreatment.

1. Introduction

Subarachnoid hemorrhage (SAH) is a common and severe cerebral accident, which accounts for 5% of all cerebral apoplexy (Yan et al., 2015). The incidence of SAH in China is about high (Zhang et al., 2013) and the mortality and disability rate is above 50% (D'Souza, 2015). The incidence of cerebrovascular spasm (CVS) after the cerebral accident is as high as 30–90% (Crowley et al., 2008). CVS can cause sever ischemia in brain tissue, which will lead to tardive hypoxic-ischemic brain damage, and results in cerebral infarction, which is the major cause mortality and disability rate (Fujii et al., 2013). However, the pathogenesis of CVS after SAH is currently unclear. Current belief holds that it is a process consisting of many factors and complexed networks of events like oxidative damage, bioenergetics and cell death (Danura et al., 2015; Rodriguez-Rodriguez et al., 2014). The current of potassium ion channel changes in the early stages after SAH, which may trigger CVS. The ATP sensitive K^+ channels (sK_{ATP}) are related to cell metabolism and membrane excitability, in vascular smooth muscle cells. sK_{ATP} channel of membrane potentially plays a significant role in the regulation of vascular tension (Nelson et al., 1990). sK_{ATP} open channel can cause smooth muscle cell membrane hyperpolarization, and a reduction of Ca^{2+} through the voltage-dependent calcium channel (VDCCs) flow channel, causing vasodilation. In addition, the drugs activating sK_{ATP} increase K + outflow, which can cause membrane hyperpolarization and vascular smooth muscle relaxation(Quast et al., 1994). Smooth muscle sK_{ATP} channel is a common molecular target of many vasodilators and plays an important role in vasodilation.

A burst of pro-inflammatory cytokines and chemokines were released from various cells including smooth muscle cells in the artery after SAH (Takizawa et al., 2001). This early molecular event triggers of recruitment of immune cells to the injured area and leads to a significant cause of oxidative damage (Yang et al., 2017). There is no

* Corresponding author.
E-mail address: shixianqing@126.com (X. Shi).

https://doi.org/10.1016/j.fct.2019.110804
Received 13 June 2019; Received in revised form 17 August 2019; Accepted 4 September 2019
Available online 07 September 2019

literature linking co-occurrence of the oxidative damage with changes either in functional or morphology of basilar artery and smooth muscle sK_{ATP} channel. This is the goal of this present study. Many small molecule such as cannabinoids have immense effect on transcriptional regulation and control many physiological responses (Mukhopadhyay et al., 2015). Shikonin is a Chinese traditional medicine and have a beneficial effect in various disease models via anti-inflammation, antioxidant and anti-cancer (Boulos et al., 2019; Chen et al., 2003, 2011; Guo et al., 2019; Liu et al., 2019; Park et al., 2013; Tanaka et al., 1986; Yu et al., 2019).

Using the rabbit SAH model, our research focused on the relationship between sK_{ATP} channel current change and CVS during early SAH, to find the best time window for prevention and treatment of early CVS after SAH. The therapeutic potential of shikonin in SAH was also evaluated.

2. Method

2.1. Experimental design

New Zealand white rabbits (both male and female) provided by the animal center of HuaXi Basic Medical College of Sichuan University were randomly divided into groups with 8 rabbits in each group. In SAH, rabbits were injected with non-anticoagulative arterial auto blood through the cisterna magna and samples were collected at 24, 48 and 72 h. Sham group was injected with the same amount of saline. Shikonin (50 mg/kg) or maize oil was administered in experimental group and samples were collected either at 24 or 72 h. The animal experimental protocols were approved by the Animal Care and Research Committee of Sichuan University. All procedures were conducted in accordance with the Guidance for the care and use of laboratory animals, formulated by the Ministry of Science and Technology of the People's Republic of China. All surgery was performed under anesthesia, and all efforts were made to minimize sufferings.

2.2. Experimental SAH model

SAH model was set up by injecting non-anti-coagulative arterial autologous blood through cisterna magna (Satoh et al., 2001). Briefly, rabbits were fastened on the experiment table with the prone low head position after anesthesia with an injection of 3% Nembutal (1 ml/kg) and midazolam (1 mg/kg), 150000 unit Penicillin was given to prevent infection. During the experiment, rabbits were given an oxygen mask and kept an open airway, the rectal temperature was kept at 18–40° with an electric blanket. After Shaving the hair of surgical area, sterilizing and laying sterile towels, Num 5 IV needle was slowly inserted into the suboccipital gap and 1 ml/kg non-anticoagulant arterial blood was uniformly injected into cisterna magna within 1 min, 37° saline (1 ml/kg) was injected as a control. All animals were kept at 30-degree prone position for 30 min after injection before changed to the lateral position. Respiration rate, pulse oxygen saturation and rectal temperature were monitored during surgery, mean arterial pressure and Heart rate was monitored by inserting an arterial catheter into ear middle artery as well.

2.3. Isolation of basilar artery smooth muscle cells

Basilar artery smooth muscle cells were isolated based on earlier published methods (Ishiguro et al., 2005). The rabbits were sacrificed at 24h, 48h, and 72h following SAH. The basilar arteries were isolated under a microscope, small branches of blood vessels, endothelia, the arachnoid and perivascular connective tissue were removed. The basilar arteries were cut into 1 mm square pieces. The small pieces of the basilar artery were put into the enzymatic solution I (papain 0.5 mg/ml and dithioerythritol (DTE) 1 mg/ml), and then put into the 37 °C water bath for 20 min. Next, the enzymatic solution I was replaced by enzymatic solution II with collagenase 1 mg/ml (Type XI) for 30 min in a 37 °C water bath. The digestion was stopped by removing the enzymatic solution and put into DMEM culture media with 10% cell culture tested BSA. To obtain a large number of single smooth muscle cells, the digested basilar arteries were washed repeatedly with 4 °C extracellular fluid by Pasteur pipette to release the single smooth muscle cell, the isolated cell suspension can be kept into 4 °C, and can be used for patch clamp experiment within 6h.

2.4. Cell patch

The coverslips were cleaned with clean silk textiles before cell patch and pasted onto 3.5 mm culture dishes with sealing glue on the edge, the tweezers were used to lightly press the coverslips to ensure it was fixed correctly. The cell suspension was dropped onto coverslips by the Pasteur pipette and kept at 1h, and then it was perfused 2 to 3 times with extracellular fluid at a speed of 2 ml/min to substitute PBS solution and get rid of the impurity in the cell suspension. The isolated smooth muscle cells were detected under an inverted phase-contrast microscope. The shape of the isolated smooth muscle cells was long spindle and oval with the smooth and intact cell membrane, neat of cell edge, high refractive index, uniform cytoplasm and stretching well.

2.5. Microelectrode making

The 7.5 mm (1.5 mm internal diameter, 1.10 mm external diameter) borosilicate glass tube with filament was pulled into two symmetrical glass microelectrodes by microelectrode puller (SUTTER INSTRUMENT, P-97). The solution for filling microelectrode was stored in a cold foam box containing crushed ice to prevent the degradation of ATP electrodes, and then it was filled into the tip of the microelectrode up to the edge of 1/3 of the electrode to cover the silver electrode, tapping the pipe wall to remove bubbles in the water. The electrode resistances was 5–10M Ω.

2.6. Whole-cell patch clamp recording

The whole cell patch clamp recorded the ATP sensitive potassium channel current of artery smooth muscle cells in each group. Whole-cell current amplitude (PA) and membrane capacitance (PF) were recorded, which calculated the current density (PA/PF) and drew current-voltage (I -V) curve. The reversal membrane potential (Vrev)) and membrane conductance (G) with corresponding voltage (TP) were obtained by linear fitting curve, G = I/(Vm-Vrev), I and Vm was the current peak of each TP and the voltage tested respectively. The maximum conductance (Gmax) was calculated by Gmax = Imax/(VM-Vrev). Using the (G/Gmax) as y-axis and the tested voltage (Vm) as X-axis, the scatter gram and steady-state activation curve was obtained. At last, the Boltzmann Formula was formed by fitting steady-state activation curve with the scatter gram (setting f (V) = G/Gmax, Imax = 1, Vmid = V0.5, V = Vm, Vc = k, C = 0). Which was used to obtain semi-activation voltage (V0.5) and slope factor (k)?

The peak of whole-cell current (I) was measured by testing different impulse. The maximum peak (Imax) was utilized to standardize the current under different impulse voltages, by which the relative current amplitude I/Imax was obtained, using I/Imax as Y-axis and voltage tested(Vm) as X axis to draw scatter gram and steady-state inactivation curve, they were fitted and formed the Boltzmann Formula (f(V)=I/Imax, Imax = −1, $V_{mid} = V_{0.5}$, V = Vm, Vc = k, and C = 1). The half-inactivation voltage ($V_{0.5}$) and slope factor (k) were obtained from nonlinear fitting of Boltzmann formula. Finally, glibenclamide was added into the extracellular fluid and the change of the current channel was observed.

The isolated basilar artery smooth muscle cells with the smooth, intact membrane, neat edge, stretching well, high refractive index and

uniform cytoplasm were chosen for patch clamp. The Intracellular fluid was injected into microelectrode by the injector with 0.22 μm filter, the glass electrode full of intracellular fluid was put on the propeller and moved by 3D Manipulator so that it's tip closed to the target cell. Under high magnification microscope, the electrode was gently pushed onto the surface of the cell, and the appropriate resistance (1GΩ and above was chosen) between the surface of electrode and cell was formed by exerting a little negative pressure. After the rupture of membrane, whole cell record was formed by capacitance and series resistance compensation.

Clampex 10.0 software was used to release stimulation and collect signal of all currents recorded. The current signal was guided by electrode Ag/AgC1 and amplified by Axopatch 200B amplifier (AXON INSTRUMENTS, USA), and then was input onto computer by the digital-analog converter (Digidata 1440A, AXON INSTRUMENTS, USA), Clampfit 10.0 software was used to analyze data. After whole cell recording model completed, Clampex 10.0 software was run with voltage clamp model to record cell membrane capacitance, and was used to output stimulant signals and record the K_{ATP} current after compensation for membrane capacitance and electrode capacity, the Stimulus parameters were set as holding potential was 80Mv, testing potential increased from 70 mV to 110 mV, Stride length 15 mV, Time-histories 400 ms, and frequency 0.1Hz. Utilizing current (pA/pF) with membrane potential to form the current and voltage curve. Data was collected with 5 kHz frequency after whole cells current transferred by current-voltage and low pass filtering with 1 kHz, the linear leak and incomplete compensation membrane current were subtracted with P/4. In order to assess the characteristic of sK_{ATP} channel steady-state inactivation, the peak sK_{ATP} of the whole cell (I) induced by different types of impulses were tested. HP was set at −80mv and gradually increased from −120mv to +40mv with 10mv/step, amplitude with 400 ms. HP decreased to 10 ms following increased to +40mv to create TP, which lasted 250 ms before returning to HP, and the stimulus interval was 10s.

2.7. Basilar artery pathological examination

Basilar artery tissue was taken from rabbits in each group (the coronal section was taken from 2 to 4 mm of post optic decussation and 2 mm of cerebral anterior basilar bifurcation point) for prepared for HE staining. The HE-stained picture of Basilar artery was taken under a microscope with a magnification of 40X, the luminal area and diameter were analyzed and calculated using America Image-ProPlus professional image analysis and processing software system.

2.8. Isolation of RNA and real-time PCR

RNA was isolated from basilar artery homogenate according to the manufacturer's protocol (Qiagen RNeasy Mini Kit, Qiagen, Hilden, Germany). Total RNA was subsequently converted into cDNA and Real-time PCR was carried under standard conditions with 200 pM PCR primers. Each sample was analyzed in triplets using SYBR green (Applied Biosystems) as fluorescent detector and GAPDH as an endogenous control. All primers were obtained for RT qPCR Primer assay were published earlier (Yang et al., 2014).

2.9. Co-immunoprecipitation and immunoblot analyses

Proteins from perforation side tissue samples were isolated by lysing in RIPA buffer with protease inhibitor cocktail (Roche) and quantified as described earlier (Shi et al., 2017). Co-immunoprecipitation were performed as described earlier (Zhou et al., 2019). Equal amount of proteins was loaded onto gel, transferred into nitrocellulose membrane, blocked with 10% nonfat milk in PBS-Tween20. Membranes were incubated with antibodies TNFα, IL1β, β-actin (Biomatik, Ontario, Canada) ZO1, Occludin (LS Bio, Seattle, USA), protein nitration (Cayman Chemical,Ann Arbor,USA). After two washing with PBS-Tween20, the membrane was incubated with corresponding secondary antibodies (Beyotime, Shanghai, China) followed by chemiluminescence detection.

2.10. Protein nitration

Protein nitration was measured from basilar artery lysate in sham, and experimental groups by ELISA kit (Bioswamp, China), according to the manufacturer's instructions.

2.11. PARP activity

PARP activity from basilar artery lysate samples was measure as described earlier (Putt et al., 2005).

2.12. Data analysis and statistics procession

Data were presented as mean ± standard deviation, comparison of intragroup and different groups were processed by the *t*-test and One - Way ANOVA analysis respectively, $P < 0.05$ showed the difference was statistically significant.

3. Results and discussion

3.1. Time-dependent alterations of physiological parameters after SAH in rabbit

Dark red blood clots around of posterior basal pool and partially adhered arachnoid were examined in animals after SAH (Supplemental Table 1). Before SAH, each of the rabbit weight showed no significant differences ($P > 0.05$), but the weight of 24h–72h group significantly decreased after SAH injury. There was no significant difference in heart rate (HR) and mean arterial pressure (MAP) in each group before and after modeling (Supplemental Table 1).

Intracranial vascular puncture easily damages brain tissues and increases the risk of bleeding due to severe damage, and results in the death of rats, with a mortality rate ranging from 16% to 44%(Gao et al., 2008). Single intracisternal blood injection was shown that can form more blood clots surrounding basilar artery and was feasible and reliable for replicating SAH model. By which, the pathological process of SAH was vividly simulated, simple in operation and easy in the control of bleeding. Additionally, no complex vascular network bridging the internal and external circulation of the brain in rabbits, the vessel type of rabbit is much closer to that of humans than cat and dog. Therefore, the rabbit SAH model was adopted in this experiment.

The weights of rabbits decreased after SAH which may be caused by loss of appetite and decreased intake of food due to the feeding center suppressed resulting from the insufficient blood supply, following the cerebral vasospasm induced by hemorrhage.

3.2. Induction of pro-inflammatory cytokines/chemokines peak at 24h after SAH

We observed significant induction of pro-inflammatory cytokines at 24h after SAH and gradually decreased at 72h. Pro-inflammatory cytokines IL-22, IL1β, and TNFα all increased significantly at 24,48 and 72 h after SAH (Fig. 1a–c). IL-22 have shown a crucial role in West Nile encephalitis pathogenesis and endothelial dysfunction (Wang et al., 2012; Ye et al., 2017). Both TNFα and IL1β are elevated in the early stage of SAH in human and mice models (Chou et al., 2012; Sozen et al., 2009). We also observed an increase of CXCL3 chemokine in the same pattern (Fig. 1d) as the other cytokines and in accordance with the mice model of SAH (Shi et al., 2017). Two of the cytokines IL1β and TNFα were verified at the protein level by immunoblot analyses (Fig. 1e). The pro-inflammatory response is critical for the recruitment of immune cells and repair of damaged arteries.

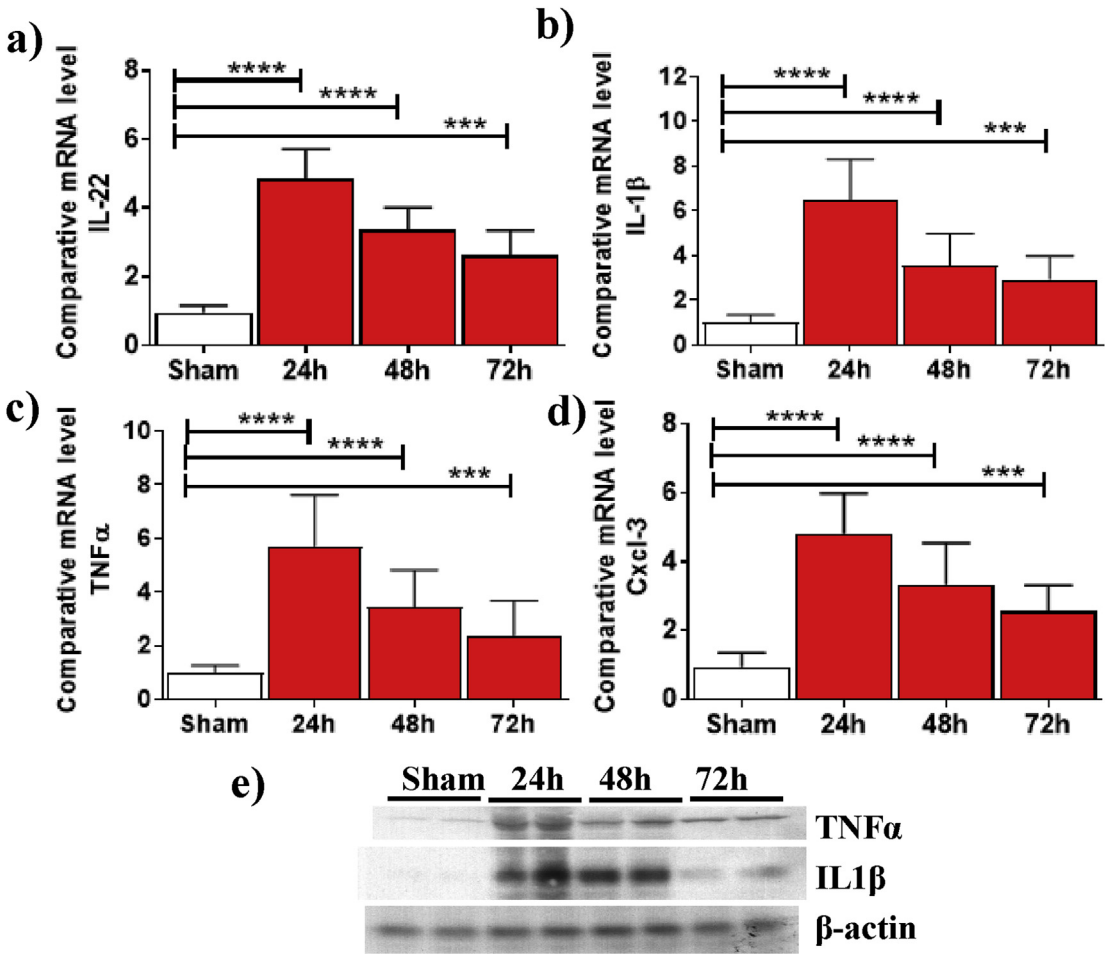

Fig. 1. Time-dependent studies on inflammatory response after SAH. Pro-inflammatory cytokines/chemokine IL-22 (a), IL1β (b), TNFα (c) and CXCL3(d) were induced at 24h after SAH and gradually decreased up to 72h compared to sham. Values are mean ± standard deviation and statistically compared to the sham group; N = 8/group, **** represents $p < 0.0001$ and *** represents $p < 0.001$. e) Immunoblot analyses of two cytokines TNFα and IL1β with loading control β-actin.

3.3. Induction of oxidative damage and morphological changes in basilar artery peak at 72h after SAH

The oxidative damage measured by protein nitration of basilar arteries and cell death marker total PARP activity was increased from 24h to 72h (Fig. 2a and b). PARP is a key measure of cellular damage and pharmacological intervention of PARP lead to protection in SAH (Satoh et al., 2001). Compared with the sham operation group, the basilar artery area, and diameter of the SAH group were smaller and was significantly different. In SAH group, the lumen area and diameter of the 72h group were smaller than that of 48h and 24h group (Fig. 2c and d). It is obvious that the maximum oxidative damage was related to maximum damage to the morphology of basilar arteries.

3.4. Significant alteration of the molecular function in ATP sensitive potassium channel of isolated basilar artery smooth muscle cell at 72h after SAH

The isolated basilar artery smooth muscle cells in five random visual fields under high magnification microscope were detected and counted, results showed it is no significant different in cell numbers between groups. The morphology of majority cells detected under inverted phase contrast microscope is long shuttle and partial cell presented as the oval, with the integrity cell membrane, high refractive index, and uniform cytoplasm. There is no difference in the sizes of cells in every group.

This experiment adopted two-step enzyme (Papain and type XI collagenase) digestion method for acute separation of BASMCs, and it only took about 60min in the whole process, from vascular separation to the digestion into single BASMC cells in the shapes of long fusiform or ovals, and there was no obvious difference between groups in the number of cells. Cell membranes were intact, with smooth surfaces, high refractive index, uniform cytoplasm, high survival rate and easy to form high resistance seals with a glass electrode, to meet the needs of patch clamp test (Fig. 3a). The cell membrane ruptured and formed a high resistance seals after the formation of the whole cell recording mode, 20 cells were randomly selected from each group to record the cell membrane capacitance (Cm), the results showed that there were no significant differences in membrane capacitance between groups (Table 1), which suggested that there is no significant difference in cell size. Basilar artery smooth muscle cells of the sealing process were shown in Fig. 3b. To verify whether the reduced current is sK_{ATP} current, an ATP sensitive potassium channel blocker glibenclamide was added (10μmol/), the results showed that glibenclamide could effectively inhibit the current, which indicated that the current recorded in the experiment is ATP-sensitive potassium channel current. Compared with group C, the currents of ATP-sensitive potassium channels in group 24h–72h were decreased (Table 1). In order to eliminate the influence of difference of cell size on current, the current was converted to the current density (PA/PF), and the current-voltage (I–V) curve was plotted using current density (PA/PF) and Tested potential (TP, mv) (Fig. 3c, Table 1). The numbers of ATP sensitive potassium channel

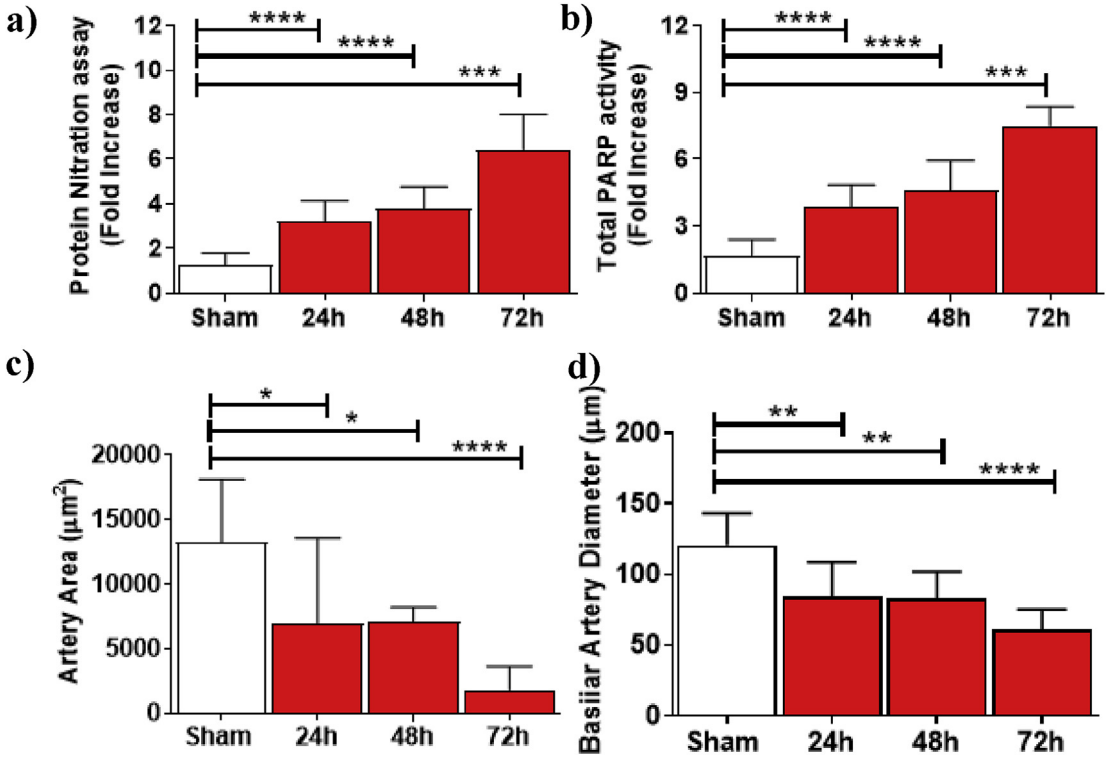

Fig. 2. Time-dependent studies on oxidative damage and arterial morphological changes after SAH. Oxidative damage measured by protein nitration(a) and cell death measured by PARP(b) were at its peak at 72h and gradually increased from 24h. Both basilar artery area(c) and diameter(d) gradually decreased at 72h in a time-dependent manner. Values are mean ± standard deviation and statistically compared to sham group; N = 8/group, **** represents $p < 0.0001$; *** represents $p < 0.001$; ** represents $p < 0.01$; * represents $p < 0.05$.

increased with the increase in voltage. Compared to the sham group, the activation curves of 24h–72h groups shifted to the right (Fig. 3c), the numbers of ATP sensitive potassium channel opened under the same voltage were reduced. The half-activation voltage (V0.5) in 24h–72h groups significantly increased compared with sham group C (Table 2), but no significant difference has shown in slope factor (k) between groups, which indicated it needs the higher voltage stimulation to open the of basilar artery smooth muscle cells after SAH but the speed of ATP sensitive potassium channel open is not affected, this results in a reduction of potassium ion efflux and the decrease of the current, which may be the important cause of vasospasm after SAH.

ATP sensitive potassium channels in vascular smooth muscle are composed of two subunits: inwardly rectifying potassium channel (Kir6.1) and sulphonylurea receptor (SUR2B) (Aihara et al., 2004; Ko et al., 2008). K_{ATP} channels can affect the contractile and diastolic function of vascular smooth muscle, maintaining the basal tension of

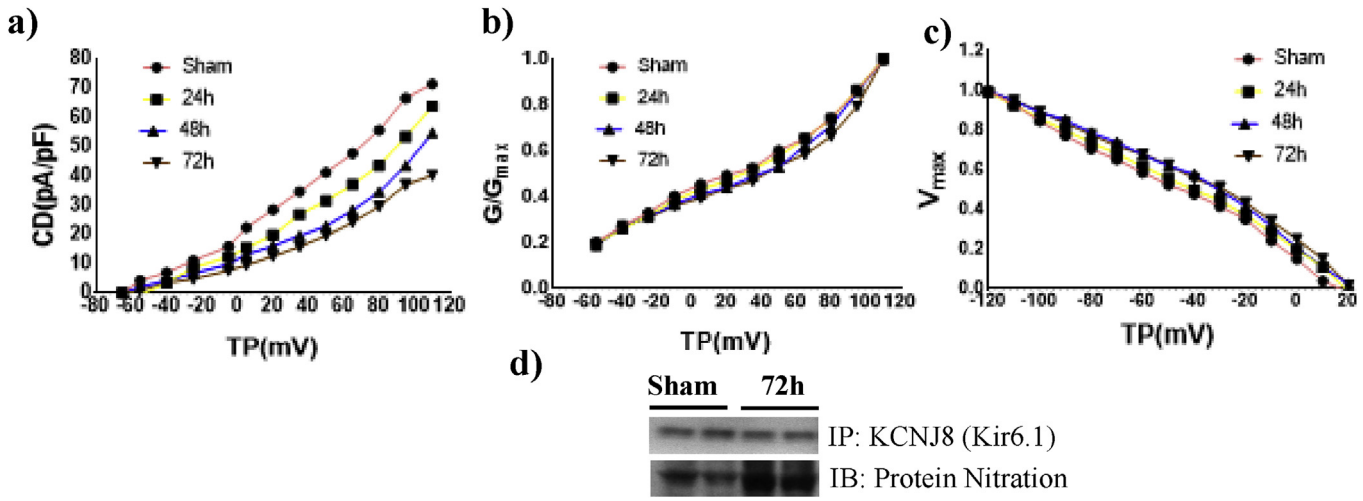

Fig. 3. Time-dependent studies current-voltage characteristic curves(I–V curve) of potassium channel after SAH. a) The pattern of I–V curves of each group is upward, and the IK_{ATP} increased with the increase of membrane potential. There is no statistical difference among sham(C), 24h(S1) and 48h (S2) in the peak of sK_{ATP} current. The peak of sK_{ATP} current at72h(S3) group was lower than that of sham group C($p < 0.05$), which indicated that the reduction of the ATP-sensitive potassium channel of basilar artery smooth muscle cell opened at 72 h after SAH and the current decreased. b) The steady-state activation curves of the same groups as described above and are not statistically different c) The steady-state inactivation curves of the same groups as described above. d) Immunoprecipitation of perforation side tissue lysates from sham and 72h time points with KCNA1 followed by immunoblot analyses with anti-nitrotyrosine antibody.

Table 1
Comparison of Membrane capacitance(unit:PF) and peak of sK_{ATP} current.

Group	Number of cells	Membrane capacitance of cells	sKATP current(pA/pF)
Sham	20	13.86 ± 0.25	73.09 ± 33.64
24h	20	13.86 ± 0.24	60.83 ± 37.92
48h	20	13.90 ± 0.31	54.85 ± 21.28
72h	20	13.79 ± 0.30	41.41 ± 16.80[a]

[a] Is statistically significant, $P < 0.05$ (n = 8/group).

vascular bed, and activates KATP channel during ischemia and hypoxia, to dilate blood vessel and increase blood flow (Buckley et al., 2006). To understand, the effect of oxidative damage to these channel proteins, we examined oxidative modification of Kir6.1 by immunoprecipitation (Fig. 3d). Kir6.1 was significantly modified at 72h after SAH resulting altered function. sK_{ATP} channel is associated with the metabolism and membrane excitability of cells and plays an important role in the regulation of membrane potential and vascular tone in vascular smooth muscle cells. The opening of sK_{ATP} channels hyperpolarizes the membrane of the smooth muscle cell, reduces the inflow of Ca^{2+} through voltage-dependent calcium channels (VDCCs), and thus resulting in vasodilation.

Gating kinetics of sK_{ATP} channel is featured by high ATP and voltage dependency, and the opening or closing of the channel depends on the concentration of ATP and ADP in cells, while the opening degree on the membrane potential. In this experiment, no blockers of sodium channels and calcium channels were added in the extracellular solution. As sodium channel was inactivated at −40mV for 200 ms and the HP was set at −80mV in this experiment, when sodium ions changed from resting state to inactive state and took a long time to restore to resting state from inactivated state. As it was difficult for sodium ions to restore to be resting state during the period of voltage testing, the current in the sodium channel was not recorded. Compared to the current in potassium channel, the current in calcium channel was smaller and inactivated quickly, so it did not affect the measurement of current in the potassium ion channel. In the case of normal extracellular Ca^{2+} concentration, the maximum current was smaller than 50 pA and lasted for about 30 ms, so it had little effects and thus not blocking calcium ion channel, and blockers, because of its toxic properties, affected the recording. In order to identify whether the outward current recorded was generated in ATP sensitive potassium channel, glibenclamide, specific ATP sensitive potassium channel blocker, was added in cell bath, showing that glibenclamide effectively inhibited currents generated in the channel, which indicated that current recorded was generated in ATP sensitive potassium channel.

The experimental results showed that the sK_{ATP} current of group 72h was smaller than that of sham group and there was no significant difference in sK_{ATP} current between sham group with group 24h or group 48h (Table 1), suggesting that the development probability of ATP sensitive potassium channel of rabbit basilar artery smooth muscle cells at 72h after SAH lowered, or protein expressing decreased. This showed that after receiving the same level of suprathreshold stimulation, the current passing through sK_{ATP} was much less at 72h after SAH than other groups, resulting in increased contractile response of smooth muscle cells. Foreign studies showed that the sK_{ATP} channel activator-levcromakalim increased basilar artery vasodilation of rabbits 3 days after SAH (Zuccarello et al., 1996) and basilar arterial vasodilation of dogs 7 days after SAH (Sugai et al., 1999), consistent with the conclusion made in this experiment that currently passed through sK_{ATP} decreased 72h after SAH. The results showed that the basilar artery smooth muscle cell sK_{ATP} was abnormally closed or protein expression decreased after SAH, the efflux of potassium ion decreased, and the current passing through this channel decreased, thus promoting the contraction of smooth muscle and causing CVS.

Ion channel activation curve reflects the speed and difficulty degree of channel opening. As shown in Table 2, with the increase of voltage, the number of ATP sensitive potassium channel to be opened is on the increase, and the activation curves of group 24h–72h were to the right of that of sham group, indicating that the number of channels to be opened under the same voltage decreased; it can be hypothesized from Table 2 that semi-activated voltage of group 24h–72h (V0.5) and sham group were relatively high. Compared with sham group, the slope factor (k) of each group does not change significantly, indicating that compared to the control group, ATP sensitive potassium channel of basilar artery smooth muscle cells after SAH opened under the stimulation of high voltage, but the opening speed of the channel is not affected (K value does not change significantly). This may be related to the change of the function of sK_{ATP} after SAH, which reduces the activity of the channel and makes the channel open under a higher level of suprathreshold stimulation. The difficulty in the opening of the channel reduces the outflow of potassium ions, resulting in the contraction of smooth muscle. The results of the experiment suggested that the sK_{ATP} current in basilar artery smooth muscle cells after SHA decreased significantly, which further demonstrated that sK_{ATP} played an important role in the development and progression of CVS.

We also observed that with the increase of voltage, the number of inactivated ATP sensitive potassium channel reduces (Table 2), and the inactivation curves of groups 24h–72h were to the right of that of the sham group C, indicating that inactivated ATP sensitive potassium channels from group 24h–72h group are more than those of sham group under the same voltage, the outflow of potassium ions decreases, similar to the current density and the changes of sK_{ATP} SAH and activation characteristics to 72h.

Based on activation and inactivation characteristics of sK_{ATP}, it concluded that compared with the control group, the sK_{ATP} current of each group after SAH reduced, and the channel was difficult to be activated and easy to be inactivated, indicating that ATP sensitive potassium channel and its function were inhibited after SAH. In consistent with earlier publications, ATP potassium channel activators acting on subarachnoid hemorrhage can effectively inhibit and alleviate cerebral vasospasm, preventive administration of ATP sensitive potassium channel activators can effectively prevent SAH-induced cerebral vasospasm. The I–V curve is not consistent with the activation curve and inactivation curves, which may be due to less experimental samples or gradually increased suppression to ATP sensitive potassium channel

Table 2
Comparison of voltage of half-activation($V_{0.5}$)and slope factor for (k) activation voltage of half-inactivation($V_{0.5}$)and slope factor for (k) activation.

Group	ATP sensitive potassium channel		Inactivated ATP sensitive potassium channel.		sK_{ATP} current (pA/pF)
	V0.5	k	V0.5	k	
Normal	16.96 ± 4.27	52.88 ± 5.21	−46.58 ± 2.63	28.29 ± 2.56	72.53 ± 28.85
Sham	15.51 ± 4.42	53.79 ± 5.44	−44.83 ± 2.28	28.05 ± 2.21	73.09 ± 33.64
24h	20.28 ± 5.95[a]	54.55 ± 6.16	−42.01 ± 1.94[a]	29.97 ± 1.94	60.83 ± 37.92
48h	25.25 ± 5.18[a]	52.67 ± 6.30	−35.18 ± 1.91[a]	28.18 ± 1.88	54.85 ± 21.28
72h	25.11 ± 5.64[a]	58.48 ± 7.38	−34.04 ± 1.81[a]	30.23 ± 2.03	41.41 ± 16.80[a]

[a] Is statistically significant, $P < 0.05$ (n = 8/group).

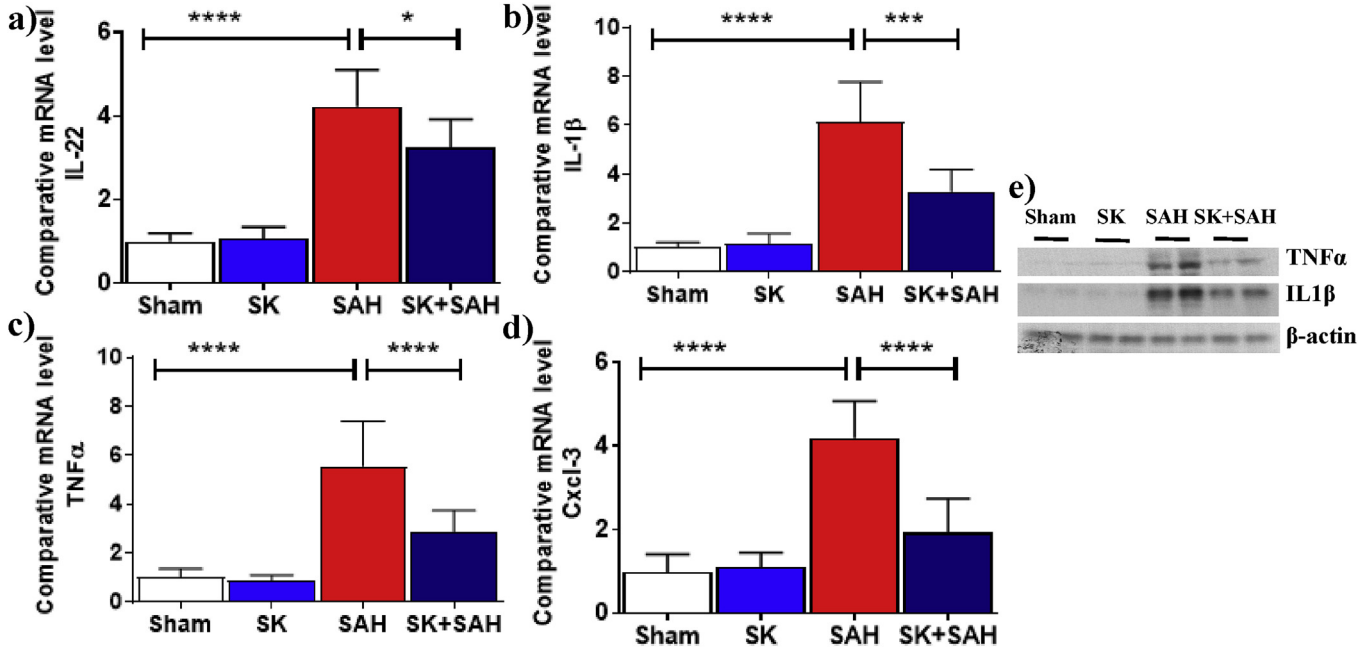

Fig. 4. Effect of Shikonin on pro-inflammatory cytokines/chemokines at 24h after SAH in the basilar arteries. Shikonin (SK) pre-treatment attenuated pro-inflammatory cytokines/chemokines IL-22(a), IL1β (b), TNFα (c) and CXCL3 (d) induced by SAH. Values are mean ± standard deviation and statistically compared to sham group or SAH group as presented; N = 8/group, **** represents $p < 0.0001$; *** represents $p < 0.001$; * represents $p < 0.05$. e) Immunoblot analyses of two cytokines TNFα and IL1β from same set of samples used for real-time PCR.

after SAH. Therefore, some experiments showed that the sK_{ATP} channel activator levcromakalim increased basilar artery vasodilation of rabbits in 3 days after SAH and basilar artery vasodilation of dogs in 7 days after SAH. But the efflux of potassium decreased after in 72h after SAH, indicating that the treatment of subarachnoid hemorrhage by drugs take effect at least 72h after SAH. In the comparison between groups in terms of lumen area and diameter of the basilar artery, lumen areas and diameters of basilar arteries of all SAH group were smaller than those of the sham operation group suggesting that change of calcium currents is related to SAH-induced early cerebral basilar artery spasm.

3.5. Protective effect of shikonin in SAH injury by reducing the early inflammatory response, oxidative stress and morphological changes to basilar arteries

Pretreatment of shikonin at 50 mg/kg to rabbit before SAH attenuated secretion of pro-inflammatory cytokines/chemokines IL-22, IL-1β, TNFα and CXCL3 at 24h as determined by real-time PCR (Fig. 4a–d). Protein levels of TNFα and IL-1β shown by immunoblot analyses also validated real-time PCR data (Fig. 4e). Shikonin pretreatment also reduced reactive oxygen species generating sources NOX2 and NOS2 determined at 72h after SAH (Fig. 5a and b). As expected shikonin attenuated both protein nitration and total PARP activity significantly at 72h after SAH in basilar arteries (Fig. 5c and d). Based on earlier time course studies, the inflammatory response was highest at 24h after SAH whereas oxidative response was highest at 72h. We used those peak time points for understanding the protective role of shikonin in SAH model. The earlier publication also demonstrated the critical role of NOX2 and NOS2 in SAH injury (Iqbal et al., 2016; Zhang et al., 2017). Shikonin reduced both oxidative damage and associated cell death after SAH. Shikonin has a direct role in scavenging reactive oxygen species (Yoshida et al., 2014) and modulation of NOX2 (Kazumura et al., 2016). In recent years, numerous publications demonstrate the immune-modulatory effect of shikonin including brain inflammation (Koike et al., 2016; Liang et al., 2016; Tanaka et al., 1986; Wang et al., 2014; Zorman et al., 2016).

The major protective effect of shikonin effect was a significant improvement of arterial morphology at 72h after SAH (Fig. 6a and b). The role of shikonin were further investigated using blood brain barrier (BBB) proteins, which are key to inflammatory cell infiltration. Shikonin pretreatment significantly improved protein level of both ZO1 and occludin (Fig. 6C) in BBB, thus improving the outcome. These protective effects were evident from reduced inflammatory response followed by reduced oxidative damage. Oxidative modulation of potassium channels and cellular dysfunction is well established (Sahoo et al., 2014). The vascular dysfunction and cell death due to altered potassium channel was one of the major contributor to morphological changes in basilar arteries after SAH and shikonin protected against those processes (Fig. 6d).

4. Conclusion

Inflammation and oxidative damages induced by SAH injury lead to many cellular dysfunctions including ATP sensitive potassium channel and associated vascular dysfunction and cell death. ATP sensitive potassium channel plays an important role in the incidence and development of SHA-induced CVS, and the abnormal changes of ATP sensitive potassium channel after SAH and decreased efflux of potassium diminished current generated in ATP sensitive potassium channel, to promote the contraction of vascular smooth muscle cells and induce cerebral vasospasm, which may be one of the mechanisms underlying SAH-induced CVS. Shikonin improved both inflammatory response, oxidative damage, blood brain barrier function and thus improving basilar arteries structural changes, possibly ATP sensitive potassium channel and preventing cell death.

Declaration of competing interest

The authors declare that they have no known competing financial interests or personal relationships that could have appeared to influence the work reported in this paper.

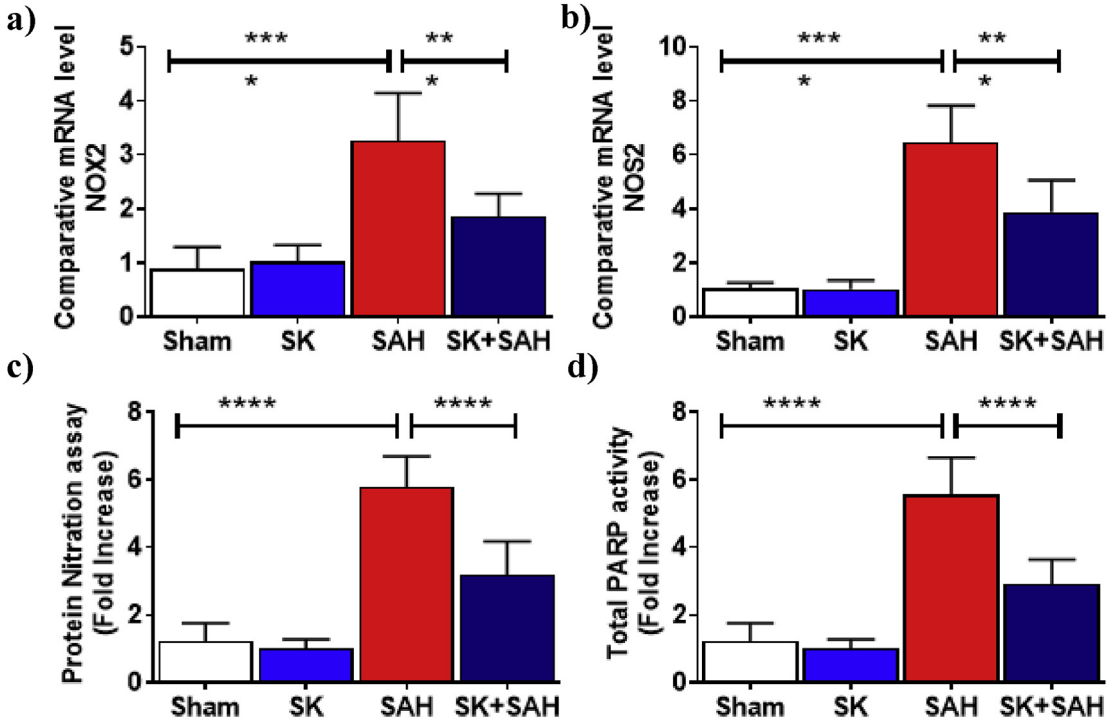

Fig. 5. Effect of Shikonin on reactive oxygen generation sources, oxidative damages and cell death at 72h after SAH in the basilar arteries. Shikonin (SK) pre-treatment attenuated two major reactive oxygen sources NOX2(a) and NOS2(b) resulting in reduced oxidative damage(c) and cell death marker total PARP activity(d) induced by SAH. Values are mean ± standard deviation and statistically compared to the sham group or SAH group as presented; N = 8/group, **** represents $p < 0.0001$.

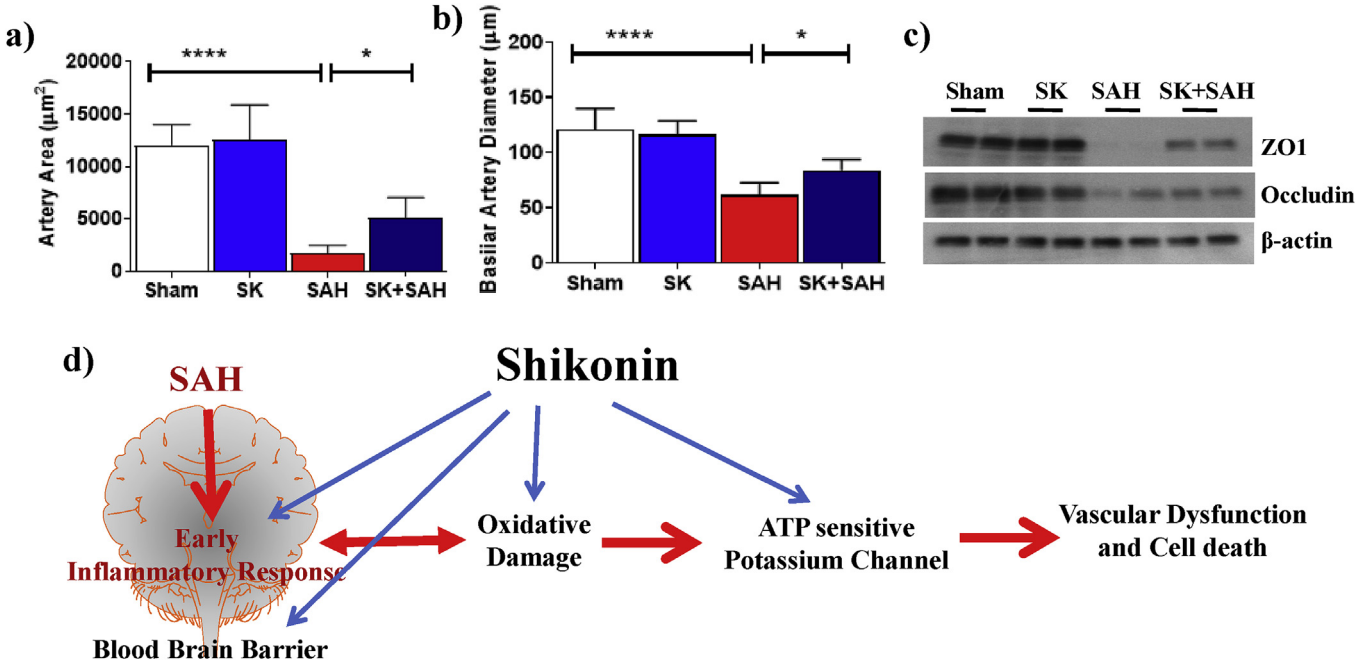

Fig. 6. Effect of Shikonin on morphological changes in basilar arteries at 72h after SAH. Shikonin (SK) pre-treatment attenuated morphological changes of basilar artery area(a) and diameter(b) induced by SAH. Values are mean ± standard deviation and statistically compared to a sham group or SAH group as presented; N = 8/group, **** represents $p < 0.0001$; * represents $p < 0.05$. c) Immunoblot analyses of blood brain barrier proteins ZO1 and Occludin with loading control β-actin d) Schematic representation of the mechanistic role of Shikonin protection at multiple levels in SAH model of rabbit.

Acknowledgement

This work was supported by Guizhou Science and Technology Department [2016]1095, Doctor foundation of Guizhou provincial people's hospital (No.GZSYB[2016]09),Cultivating foundation of Guizhou provincial people's hospital Science Foundation of China ([2018]5764-09).

Appendix A. Supplementary data

Supplementary data to this article can be found online at https://doi.org/10.1016/j.fct.2019.110804.

Transparency document

Transparency document related to this article can be found online at https://doi.org/10.1016/j.fct.2019.110804.

References

Aihara, Y., Jahromi, B.S., Yassari, R., Nikitina, E., Agbaje-Williams, M., Macdonald, R.L., 2004. Molecular profile of vascular ion channels after experimental subarachnoid hemorrhage. J. Cereb. Blood Flow Metab. 24, 75–83.

Boulos, J.C., Rahama, M., Hegazy, M.F., Efferth, T., 2019. Shikonin derivatives for cancer prevention and therapy. Cancer Lett. 459, 248–267.

Buckley, J.F., Singer, M., Clapp, L.H., 2006. Role of KATP channels in sepsis. Cardiovasc. Res. 72, 220–230.

Chen, J., Xie, J., Jiang, Z., Wang, B., Wang, Y., Hu, X., 2011. Shikonin and its analogs inhibit cancer cell glycolysis by targeting tumor pyruvate kinase-M2. Oncogene 30, 4297–4306.

Chen, X., Yang, L., Zhang, N., Turpin, J.A., Buckheit, R.W., Osterling, C., Oppenheim, J.J., Howard, O.M., 2003. Shikonin, a component of Chinese herbal medicine, inhibits chemokine receptor function and suppresses human immunodeficiency virus type 1. Antimicrob. Agents Chemother. 47, 2810–2816.

Chou, S.H., Feske, S.K., Atherton, J., Konigsberg, R.G., De Jager, P.L., Du, R., Ogilvy, C.S., Lo, E.H., Ning, M., 2012. Early elevation of serum tumor necrosis factor-alpha is associated with poor outcome in subarachnoid hemorrhage. J. Investig. Med. 60, 1054–1058.

Crowley, R.W., Medel, R., Kassell, N.F., Dumont, A.S., 2008. New insights into the causes and therapy of cerebral vasospasm following subarachnoid hemorrhage. Drug Discov. Today 13, 254–260.

D'Souza, S., 2015. Aneurysmal subarachnoid hemorrhage. J. Neurosurg. Anesthesiol. 27, 222–240.

Danura, H., Schatlo, B., Marbacher, S., Kerkeni, H., Diepers, M., Remonda, L., Fathi, A.R., Fandino, J., 2015. Acute angiographic vasospasm and the incidence of delayed cerebral vasospasm: preliminary results. Acta Neurochir. Suppl. 120, 187–190.

Fujii, M., Yan, J., Rolland, W.B., Soejima, Y., Caner, B., Zhang, J.H., 2013. Early brain injury, an evolving frontier in subarachnoid hemorrhage research. Transl Stroke Res 4, 432–446.

Gao, C., Liu, X., Liu, W., Shi, H., Zhao, Z., Chen, H., Zhao, S., 2008. Anti-apoptotic and neuroprotective effects of Tetramethylpyrazine following subarachnoid hemorrhage in rats. Auton. Neurosci. 141, 22–30.

Guo, H., Sun, J., Li, D., Hu, Y., Yu, X., Hua, H., Jing, X., Chen, F., Jia, Z., Xu, J., 2019. Shikonin attenuates acetaminophen-induced acute liver injury via inhibition of oxidative stress and inflammation. Biomed. Pharmacother. 112, 108704.

Iqbal, S., Hayman, E.G., Hong, C., Stokum, J.A., Kurland, D.B., Gerzanich, V., Simard, J.M., 2016. Inducible nitric oxide synthase (NOS-2) in subarachnoid hemorrhage: regulatory mechanisms and therapeutic implications. Brain Circ 2, 8–19.

Ishiguro, M., Wellman, T.L., Honda, A., Russell, S.R., Tranmer, B.I., Wellman, G.C., 2005. Emergence of a R-type Ca2+ channel (CaV 2.3) contributes to cerebral artery constriction after subarachnoid hemorrhage. Circ. Res. 96, 419–426.

Kazumura, K., Yoshida, L.S., Hara, A., Tsuchiya, H., Morishita, N., Kawagishi, H., Kakegawa, T., Yuda, Y., Takano-Ohmuro, H., 2016. Inhibition of neutrophil superoxide generation by shikonin is associated with suppression of cellular Ca(2+) fluxes. J. Clin. Biochem. Nutr. 59, 1–9.

Ko, E.A., Han, J., Jung, I.D., Park, W.S., 2008. Physiological roles of K+ channels in vascular smooth muscle cells. J. Smooth Muscle Res. 44, 65–81.

Koike, A., Shibano, M., Mori, H., Kohama, K., Fujimori, K., Amano, F., 2016. Simultaneous addition of shikonin and its derivatives with lipopolysaccharide induces rapid macrophage death. Biol. Pharm. Bull. 39, 969–976.

Liang, W., Cai, A., Chen, G., Xi, H., Wu, X., Cui, J., Zhang, K., Zhao, X., Yu, J., Wei, B., Chen, L., 2016. Shikonin induces mitochondria-mediated apoptosis and enhances chemotherapeutic sensitivity of gastric cancer through reactive oxygen species. Sci. Rep. 6, 38267.

Liu, T., Sun, X., Cao, Z., 2019. Shikonin-induced necroptosis in nasopharyngeal carcinoma cells via ROS overproduction and upregulation of RIPK1/RIPK3/MLKL expression. OncoTargets Ther. 12, 2605–2614.

Mukhopadhyay, B., Schuebel, K., Mukhopadhyay, P., Cinar, R., Godlewski, G., Xiong, K., Mackie, K., Lizak, M., Yuan, Q., Goldman, D., Kunos, G., 2015. Cannabinoid receptor 1 promotes hepatocellular carcinoma initiation and progression through multiple mechanisms. Hepatology 61, 1615–1626.

Nelson, M.T., Patlak, J.B., Worley, J.F., Standen, N.B., 1990. Calcium channels, potassium channels, and voltage dependence of arterial smooth muscle tone. Am. J. Physiol. 259, C3–C18.

Park, S., Shin, H., Cho, Y., 2013. Shikonin induces programmed necrosis-like cell death through the formation of receptor interacting protein 1 and 3 complex. Food Chem. Toxicol. 55, 36–41.

Putt, K.S., Beilman, G.J., Hergenrother, P.J., 2005. Direct quantitation of poly(ADP-ribose) polymerase (PARP) activity as a means to distinguish necrotic and apoptotic death in cell and tissue samples. Chembiochem 6, 53–55.

Quast, U., Guillon, J.M., Cavero, I., 1994. Cellular pharmacology of potassium channel openers in vascular smooth muscle. Cardiovasc. Res. 28, 805–810.

Rodriguez-Rodriguez, A., Egea-Guerrero, J.J., Ruiz de Azua-Lopez, Z., Murillo-Cabezas, F., 2014. Biomarkers of vasospasm development and outcome in aneurysmal subarachnoid hemorrhage. J. Neurol. Sci. 341, 119–127.

Sahoo, N., Hoshi, T., Heinemann, S.H., 2014. Oxidative modulation of voltage-gated potassium channels. Antioxidants Redox Signal. 21, 933–952.

Satoh, M., Date, I., Nakajima, M., Takahashi, K., Iseda, K., Tamiya, T., Ohmoto, T., Ninomiya, Y., Asari, S., 2001. Inhibition of poly(ADP-ribose) polymerase attenuates cerebral vasospasm after subarachnoid hemorrhage in rabbits. Stroke 32, 225–231.

Shi, X., Fu, Y., Zhang, S., Ding, H., Chen, J., 2017. Baicalin attenuates subarachnoid hemorrhagic brain injury by modulating blood-brain barrier disruption, inflammation, and oxidative damage in mice. Oxid Med Cell Longev 1401790 2017.

Sozen, T., Tsuchiyama, R., Hasegawa, Y., Suzuki, H., Jadhav, V., Nishizawa, S., Zhang, J.H., 2009. Role of interleukin-1beta in early brain injury after subarachnoid hemorrhage in mice. Stroke 40, 2519–2525.

Sugai, K., Yaganisawa, T., Motohashi, O., Suzuki, M., Yoshimoto, T., 1999. Levcromakalim decreases cytoplasmic Ca2+ and vascular tone in basilar artery of SAH model dogs. J. Cardiovasc. Pharmacol. 33, 868–875.

Takizawa, T., Tada, T., Kitazawa, K., Tanaka, Y., Hongo, K., Kameko, M., Uemura, K.I., 2001. Inflammatory cytokine cascade released by leukocytes in cerebrospinal fluid after subarachnoid hemorrhage. Neurol. Res. 23, 724–730.

Tanaka, S., Tajima, M., Tsukada, M., Tabata, M., 1986. A comparative study on anti-inflammatory activities of the enantiomers, shikonin and alkannin. J. Nat. Prod. 49, 466–469.

Wang, L., Li, Z., Zhang, X., Wang, S., Zhu, C., Miao, J., Chen, L., Cui, L., Qiao, H., 2014. Protective effect of shikonin in experimental ischemic stroke: attenuated TLR4, p-p38MAPK, NF-kappaB, TNF-alpha and MMP-9 expression, up-regulated claudin-5 expression, ameliorated BBB permeability. Neurochem. Res. 39, 97–106.

Wang, P., Bai, F., Zenewicz, L.A., Dai, J., Gate, D., Cheng, G., Yang, L., Qian, F., Yuan, X., Montgomery, R.R., Flavell, R.A., Town, T., Fikrig, E., 2012. IL-22 signaling contributes to West Nile encephalitis pathogenesis. PLoS One 7, e44153.

Yan, H., Zhang, D., Hao, S., Li, K., Hang, C.H., 2015. Role of mitochondrial calcium uniporter in early brain injury after experimental subarachnoid hemorrhage. Mol. Neurobiol. 52, 1637–1647.

Yang, K., Zhang, X.J., Cao, L.J., Liu, X.H., Liu, Z.H., Wang, X.Q., Chen, Q.J., Lu, L., Shen, W.F., Liu, Y., 2014. Toll-like receptor 4 mediates inflammatory cytokine secretion in smooth muscle cells induced by oxidized low-density lipoprotein. PLoS One 9, e95935.

Yang, Y., Chen, S., Zhang, J.M., 2017. The updated role of oxidative stress in subarachnoid hemorrhage. Curr. Drug Deliv. 14, 832–842.

Ye, J., Ji, Q., Liu, J., Liu, L., Huang, Y., Shi, Y., Shi, L., Wang, M., Liu, M., Feng, Y., Jiang, H., Xu, Y., Wang, Z., Song, J., Lin, Y., Wan, J., 2017. Interleukin 22 promotes blood pressure elevation and endothelial dysfunction in angiotensin II-treated mice. J Am Heart Assoc 6.

Yoshida, L.S., Kohri, S., Tsunawaki, S., Kakegawa, T., Taniguchi, T., Takano-Ohmuro, H., Fujii, H., 2014. Evaluation of radical scavenging properties of shikonin. J. Clin. Biochem. Nutr. 55, 90–96.

Yu, Y.J., Xu, Y.Y., Lan, X.O., Liu, X.Y., Zhang, X.L., Gao, X.H., Geng, L., 2019. Shikonin induces apoptosis and suppresses growth in keratinocytes via CEBP-delta upregulation. Int. Immunopharmacol. 72, 511–521.

Zhang, J., Liu, G., Arima, H., Li, Y., Cheng, G., Shiue, I., Lv, L., Wang, H., Zhang, C., Zhao, J., Anderson, C.S., Investigators, C., 2013. Incidence and risks of subarachnoid hemorrhage in China. Stroke 44, 2891–2893.

Zhang, L., Li, Z., Feng, D., Shen, H., Tian, X., Li, H., Wang, Z., Chen, G., 2017. Involvement of Nox2 and Nox4 NADPH oxidases in early brain injury after subarachnoid hemorrhage. Free Radic. Res. 51, 316–328.

Zhou, L., Tang, X., Li, X., Bai, Y., Buxbaum, J.N., Chen, G., 2019. Identification of transthyretin as a novel interacting partner for the delta subunit of GABAA receptors. PLoS One 14, e0210094.

Zorman, J., Susjan, P., Hafner-Bratkovic, I., 2016. Shikonin suppresses NLRP3 and AIM2 inflammasomes by direct inhibition of caspase-1. PLoS One 11, e0159826.

Zuccarello, M., Boccaletti, R., Tosun, M., Rapoport, R.M., 1996. Role of extracellular Ca2+ in subarachnoid hemorrhage-induced spasm of the rabbit basilar artery. Stroke 27, 1896–1902.